INTERNATIONAL ATOMIC ENERGY AGENCY
20th IAEA Fusion Energy Conference
Vilamoura, Portugal, 1 - 6 November 2004

IAEA-CN-116/IT/P3-36

STUDY OF ADVANCED TOKAMAK PERFORMANCE USING THE INTERNATIONAL TOKAMAK PHYSICS ACTIVITY DATABASE

A.C.C. SIPS[1], E.J DOYLE[2], C. GORMEZANO[3], Y. BARANOV[4], E. BARBATO[3], R. BUDNY[5], P. GOHIL[6], F. IMBEAUX[7], E. JOFFRIN[7], T. FUJITA[8], N. KIRNEVA[9], X. LITAUDON[7], T. LUCE[6], M. MURAKAMI[10], J. RICE[11], O. SAUTER[12], M. WADE[10] FOR THE INTERNATIONAL ITB DATABASE WORKING GROUP, THE TRANSPORT PHYSICS GROUP OF THE ITPA AND THE STEADY STATE OPERATION GROUP OF THE ITPA.

Max-Planck-Institut für Plasmaphysik
Boltzmannstrasse 2
D-85748, Garching, Germany.

[1] Max-Planck-Institut für Plasmaphysik, Boltzmannstrasse 2, D-85748, Garching, Germany.
[2] University of California, Los Angeles, USA.
[3] ENEA Frascati Energy Research Centre, Frascati, Italy.
[4] UKAEA-EURATOM Association, Culham Science Centre, Abingdon, OX14 3DB, UK.
[5] Plasma Physics Laboratory, Princeton University, Princeton, USA.
[6] General Atomics, San Diego, USA.
[7] Association EURATOM-CEA Cadarache, St Paul lez Durance, France.
[8] JAERI, Naka Fusion Research Establishment, Naka, Japan.
[9] Kurchatov Institute of Atomic Energy, Moscow, Russia.
[10] Oak Ridge National Laboratory, Oak Ridge, Tennessee, 37831 USA
[11] Massachuchetts Institute of Technology, Cambridge, USA.
[12] Association EURATOM-Confédération Suisse, CRPP, CH-1015 Lausanne, Switzerland.

Study of Advanced Tokamak Performance Using the International Tokamak Physics Activity Database

A.C.C. Sips[1], E.J Doyle[2], C. Gormezano[3], Y. Baranov[4], E. Barbato[3], R. Budny[5], P. Gohil[6], F. Imbeaux[7], E. Joffrin[7], T. Fujita[8], N. Kirneva[9], X. Litaudon[7], T. Luce[6], M. Murakami[10], J. Rice[11], O. Sauter[12], M. Wade[10] for the international ITB database working group, the Transport Physics group[13] of the ITPA and the Steady State Operation group of the ITPA.

[1] Max-Planck-Institut für Plasmaphysik, Boltzmannstrasse 2, D-85748, Garching, Germany.
[2] University of California, Los Angeles, USA.
[3] ENEA Frascati Energy Research Centre, Frascati, Italy.
[4] UKAEA-EURATOM Association, Culham Science Centre, Abingdon, OX14 3DB, UK.
[5] Plasma Physics Laboratory, Princeton University, Princeton, USA.
[6] General Atomics, San Diego, USA.
[7] Association EURATOM-CEA Cadarache, St Paul lez Durance, France.
[8] JAERI, Naka Fusion Research Establishment, Naka, Japan.
[9] Kurchatov Institute of Atomic Energy, Moscow, Russia.
[10] Oak Ridge National Laboratory, Oak Ridge, Tennessee, 37831 USA
[11] Massachuchetts Institute of Technology, Cambridge, USA.
[12] Association EURATOM-Confédération Suisse, CRPP, CH-1015 Lausanne, Switzerland.
[13] For full list see: X. Litaudon et al *2004*, Plasma Physics and Controlled Fusion 46 (2004).

E-mail contact of the main author: ccs@ipp.mpg.de

Abstract

In recent years, an international database for advanced tokamak discharges has been constructed with data from ASDEX Upgrade, DIII-D, FT-U, JET, JT-60U, RTP, T-10, TCV, TFTR and Tore Supra. Two advanced scenarios for ITER have been studied with this scalar database: The hybrid scenario, with weak magnetic shear and q_0=1-1.5 and a steady-state scenario with reversed magnetic shear and $q_0 > q_{min}$. In this paper, previous work has been extended in three main areas: (i) The scalar data are now taken as an average over the high performance phase (before only peak values were taken), (ii) the data for the two advanced regimes can now be separated, previous studies combined all the data, and (iii) more data from DIII-D, JET and ASDEX Upgrade have been added to this new set of data for the ITPA database. The analysis in this paper concentrates on the operation space and the performance of advanced scenarios obtained so far. The hybrid scenario achieves stationary operation at high β_N ~3 operating at 50% non-inductive current fraction near the no wall beta limit ($\beta_N \sim 4l_i$). The confinement is improved over conventional H-modes, and increases with T_{i0}/T_{e0}. The data from hybrid scenario discharges show a strong correlation between the ion temperature in the core and ion temperature at the edge of the plasma. The reversed shear scenario splits into two groups of data, predominantly provided by DIII-D and JET respectively. Stationary operation has been obtained at $q_{95} \geq 5$, with the maximum performance just in line with ITER requirements for non-inductive operation at Q~5. However, this seems only possible for discharges showing a strong correlation between the core and edge ion temperature, similar to the hybrid regime. Discharges with strong internal transport barriers, although capable of achieving higher confinement, are limited to $\beta_N < 2$. Common to the two regimes is operation at ITER relevant ν^*, with the whole data set showing high confinement and peaked density profiles in this domain. The extrapolation of the results to lower ρ_i^* is hampered by the lack of sufficient input power for the largest experiments since they cannot access β_N ~ 3 at their maximum toroidal field (e.g. JET). Finally, the analysis presented here also sets the scope for further study and collaboration between experiments worldwide, co-ordinated by the ITPA.

1. Introduction

The principal reference scenario for ITER [1], a next step proposal to demonstrate fusion power as a viable energy production system, is based on H-mode operation. It provides the basis for achieving ITER's primary goal of operation at Q=10 (with Q defined as the ratio of

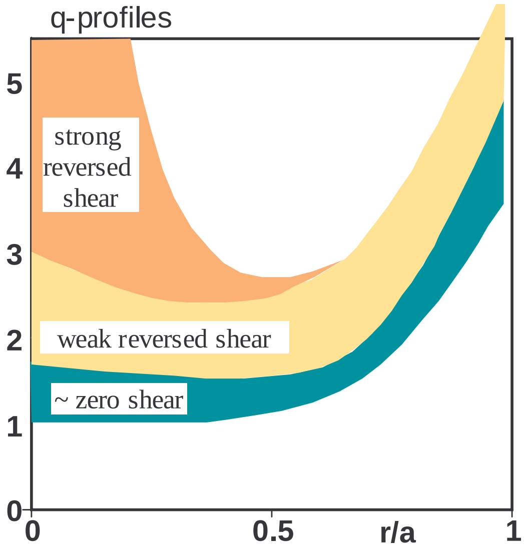

Figure 1: Classification of advanced scenarios according to the q-profile used.

fusion power to external input power). This regime relies on predictions of the baseline confinement and density parameters from an international tokamak database. Alternatively, advanced scenarios in fusion experiments seek to improve confinement and stability over standard ELMy H-modes. Key to the development of these scenarios is a tailoring and control of the current density profile. For the inductive operation mode of ITER, the safety factor profile (q-profile) is monotonically decreasing with q on axis (q_0) below unity. The safety factor at the edge (q_{95}) is near 3, determined by safe operation at maximum plasma current. Advanced scenarios use a range of (non-monotonic) q-profiles as shown in Fig. 1. It is of course possible to imagine a continuum of regimes between the reference non-inductive and inductive scenarios in which the current profile is modified externally but not completely driven by non-inductive means.

To date, two main types of advanced regimes are being developed. First, the “steady-state” advanced scenario, should provide the basis for satisfying ITER’s second major goal of reaching Q=5 under fully non-inductive conditions. This regime relies on a careful tailoring of the current density profile by external heating and current drive methods. Typically these discharges have central q above 1.5, with either weak ($|q_0-q_{min}|$ ~0.5) or strong ($q_0>>q_{min}$) reversed magnetic shear. This kind of q-profile is used to obtain internal transport barriers, which could provide sufficient bootstrap current for steady state operation. Considerable experimental time is devoted to the study of this advanced scenario in many experiments. The focus of research is on controlling the interplay of the current density and pressure profiles, to optimise the core performance. A second advanced regime, the so-called “hybrid” scenario, has a stationary current density profile with weak or low magnetic shear and q_0~1 at q_{95}~4, preventing the core sawtoothing activity. This allows operation with small m=3/n=2 neo-classically tearing modes (NTMs) at high values for normalised beta; $\beta_N = \langle\beta\rangle aB_t/I_p$ (a is the minor radius, B_t the toroidal field, I_p the plasma current). Operating at lower plasma current compared to the ITER reference scenario, this regime could lengthen the discharge duration substantially (although not steady-state).

In the next sections of this paper, a new scalar database for confinement and performance studies of advanced scenarios is presented. A survey of the performance of the two main advanced scenarios is presented (section 3). The confinement properties of these advanced regimes are given in section 4, while the operational limits in terms of achievable beta are discussed in section 5. A comparison with the ITER operational space, expressed in non-dimensional parameters, is given briefly. Conclusions and recommendations are in section 7.

2. Description of the ITPA database

Construction of an international database for advanced tokamak discharges is an activity coordinated under the International Tokamak Physics Activity (ITPA) [2]. Data from ASDEX Upgrade, DIII-D, FT-U, JET, JT-60U, RTP, T-10, TCV, TFTR and Tore Supra experiments have been collected in recent years, obtaining a comprehensive set of scalar data. In [3]

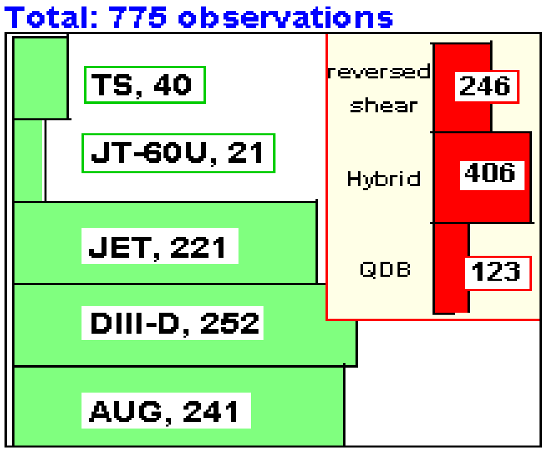

Figure 2: Overview of the new dataset.

detailed transport analysis is presented using profile data from the ITPA database. The scalar database is used to document the operational domain of the advanced scenarios and the potential use of both types of advanced scenarios in a next step such as ITER. For example, parameters are sought to better define the spatial location and occurrence, in time, of the internal transport barrier combining the data from various devices [4]. The data has also been assessed both in terms of fusion performance and capability for eventually reaching steady state [5]. The latter is based on taking the parameters at the time of maximum stored energy during the discharge, not necessarily reflecting on the stationary performance of the plasma. In the past, a proper labelling of the type of advanced scenario was not available, such that analysis of the combined data masked some of the main differences between these advanced scenarios. Moreover, 90% of the data up to 2003 was supplied from ASDEX Upgrade and JET. The data selected at present are averaged over the duration of the high performance phase, which is more appropriate for scenarios developed for long pulse or steady state operation. The duration of the high performance phase is defined as the time over which the stored energy, W, is in excess of 85% of the maximum stored energy during the pulse. Second, the total amount of discharges from ASDEX Upgrade and JET has been reduced. Previously, all attempts to make hybrids or reversed shear discharges were included; the shots removed were not advanced scenarios (failed attempts). On the other hand, more data from DIII-D are now available. The new data presented in this paper need to be submitted to the ITPA database. An overview of the data is given in Fig. 2, showing the number of data for each experiment, as well as the division of the data among the advanced regimes. Data from Quiescent Double Barrier (QDB) discharges from DIII-D have also been collected. This regime uses counter neutral beam injection to obtain a quiescent H-mode (free from ELMs), combined with an internal transport barrier to increase performance. Due to the use of counter-NBI, QDB plasmas do not presently extrapolate to steady state. As this regime has an (weak) internal transport barrier, but typically $q_0 < 1.5$ [6], these discharge do not fall firmly into one of the two advanced regimes described above, so they are treated as a separate group. Finally, in contrast to DIII-D publications, the QDB data presented here for H_{89} (and energy confinement) are uncorrected for prompt ion losses.

3. Progress towards long pulse or non-inductive operation

Obtaining stationary or steady state operation is key for advanced scenarios, but challenging as a tokamak maximises its fusion performance with inductive operation at high plasma current. Maintaining desired fusion performance (P_{fusion} ~ 400 MW for ITER) at lower plasma current implies foremost operation at higher β_N compared to the ITER reference scenario (β_N = 1.8). In addition, operation at high confinement ensures operation at high enough fusion gain ($P_{fusion}/P_{input} = Q \geq 5$ target in ITER). In the analysis below $H_{89}\times\beta_N/q_{95}^2$ is used as a figure of merit for performance: $H_{89}\times\beta_N/q_{95}^2 \sim 0.40$ for the ITER reference scenario, and $H_{89}\times\beta_N/q_{95}^2 \sim 0.3$ for the ITER non-inductive scenario. The confinement enhancement factor, $H_{89,}$ relative to ITER89P scaling is used, as this is more suited for a dataset containing discharges with a variety of edge conditions (L-mode, ELM free, H-mode with type III ELMs and H-mode with type I ELMs).

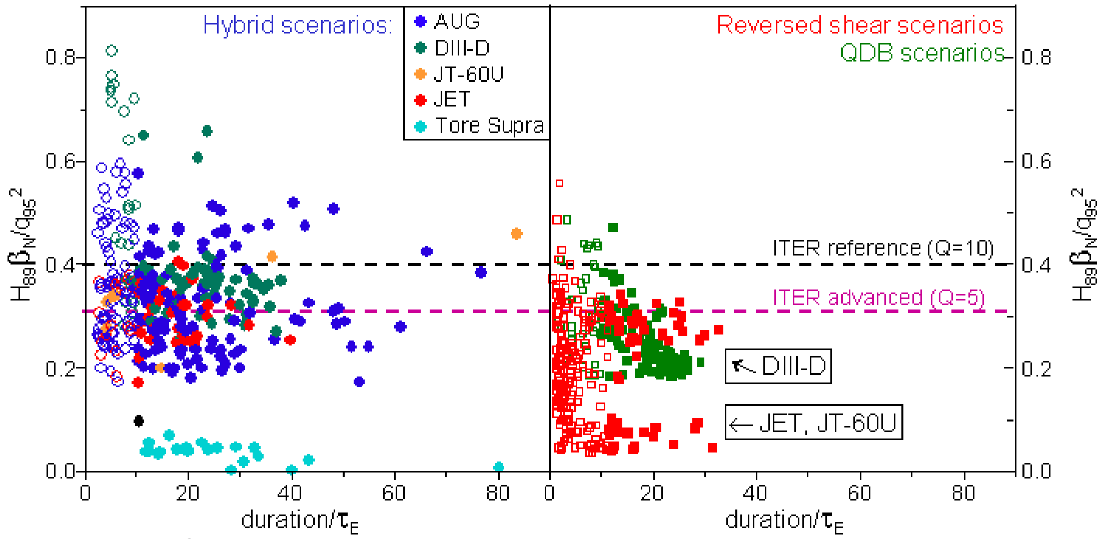

Figure 3: $H_{89}\beta_N/q_{95}^2$ versus duration (W>0.85 maximum W) normalised to the energy confinement time averaged during this time window. Hybrid scenarios are on the left and are labelled for various experiment. Reversed shear scenarios on the right and are compared with QDB data (experiments are indicated). Transient (open symbols) and stationary results (closed symbols) are given.

The results for the two regimes are plotted in Fig. 3, showing separately hybrid and reversed shear scenarios. Transient discharges (duration < $10\tau_E$) can obtain high performance, but cannot be maintained at these levels in more stationary conditions (duration ≥ $10\tau_E$). For hybrid discharges there is no clear difference between the various experiments in the dataset (only the Tore Supra data, have lower performance). Their performance achieves ITER reference values for Q~10 operation, indicating that this regime is well suited for high fluence, long pulse operation. The reversed shear results show two distinct groups, dominated by data from DIII-D, of which the best discharges come close to the ITER non-inductive advanced scenario, and data from JET (lower performance discharges).

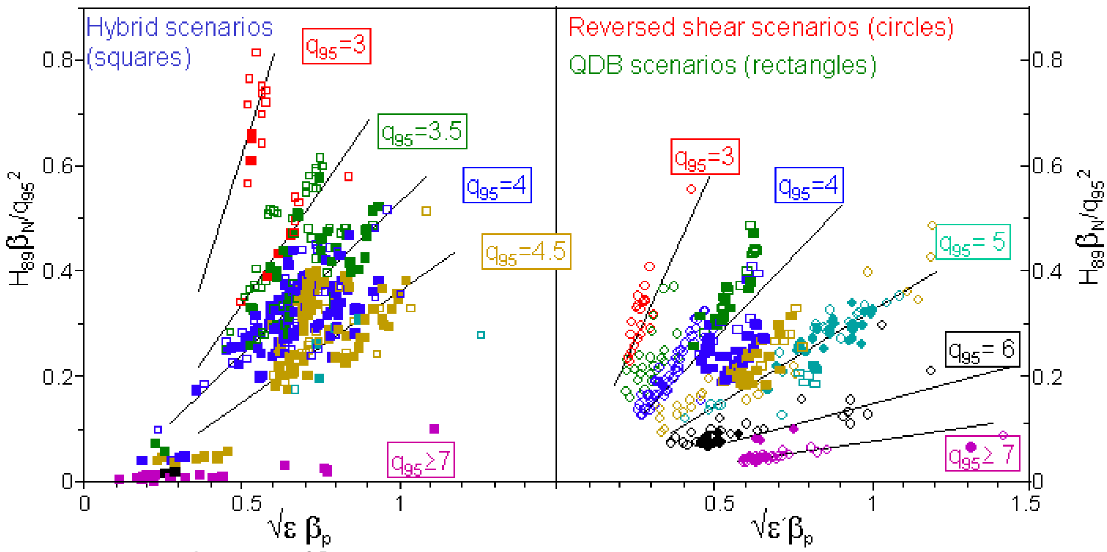

Figure 4: $H_{89}\beta_N/q_{95}^2$ versus $\varepsilon^{0.5}\beta_p$ for two different regimes: weak shear, hybrid scenarios on the left and reversed shear scenarios on the right. The colour coding indicates the different values for q_{95}, transient (open symbols) and stationary results (closed symbols) are given.

Figure 3 neither shows why there is still variation in performance nor does it indicate the ability of the regimes to provide sufficient bootstrap current. This is given in more detail in Fig. 4 where $H_{89}\times\beta_N/q_{95}^2$ is plotted versus $\varepsilon^{0.5}\beta_p$ (ε=a/R, with R the major radius,

$\beta p = 2\mu_0 \langle p \rangle / B_p^2$, with <p> the volume averaged pressure and B_p the average poloidal field). The latter is a measure for the fraction of self-generated bootstrap current for similar q-profiles; as such the two regimes are plotted separately. For hybrid scenarios, the choice is between very high performance at low q_{95}=3-3.5 (exceeding ITER reference values), or long pulse operation at q_{95}=4-4.5, were $\varepsilon^{0.5}\beta_p$ =1 implies conditions with up to 40% bootstrap fraction. For reversed shear discharges, no stationary conditions are obtained for q_{95}<5 (in contrast to QDB discharges). At higher q_{95}, values for $\varepsilon^{0.5}\beta_p$ =1 are obtained, which translate to ~65% bootstrap current fraction due to high central q values. This fulfils ITER requirements, however the results at $q_{95} \geq 6$ fail to meet the ITER performance targets.

4. Confinement and transport

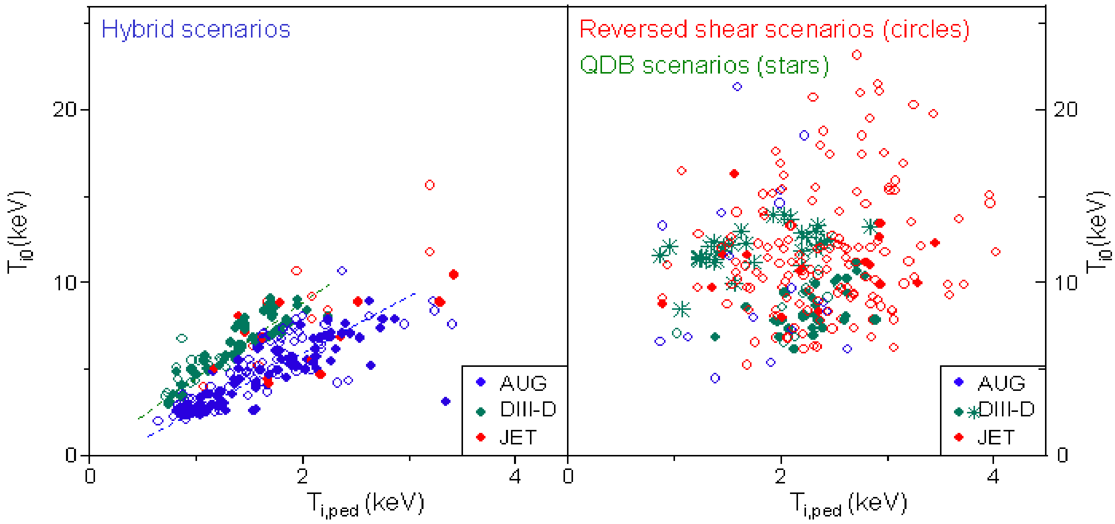

Figure 5: T_{i0} versus $T_{i,ped}$ for two different regimes., hybrid scenarios on the left and reversed shear scenarios on the right. The contribution from the different experiments is indicated. Both transient (open circles) and stationary results (closed circles) are given. QDB discharges are also presented.

Reversed shear discharges typically have internal transport barriers improving core confinement. This sets them apart from standard H-modes, which typically have stiff temperature profiles, set by a critical temperature gradient determined by turbulent driven transport. Fig. 5 shows the ion temperature in the core (T_{i0}) versus the ion temperature at 90% of the minor radius ($T_{i,ped}$) for the two advanced regimes. Clear differences are observed between the two; hybrid scenarios show a strong correlation of the core and edge ion temperatures, while reversed shear discharges show a scatter plot. This is true specifically for discharges with duration < $10\tau_E$. However, a closer look shows that most stationary discharges with reversed shear cluster around the same ratio of central to edge ion temperature as for hybrid discharges; typical for plasmas having no, or only a weak, transport barrier in the core (although a correlation between core and edge temperatures is not excluded for internal transport barrier discharges). This in itself is remarkable and indicates that the potential of an internal transport barrier, with a strong reduction of turbulent transport, cannot be fully exploited when going to steady state. This will be discussed in more detail in the next section on performance limitations. Also QDB discharges seem to have (to some extent) a fixed relation between core and edge ion temperature, although not investigated in detail here.

With hybrid pulses showing a relation between core and edge ion temperatures, also seen in conventional H-modes, the question arises as to what is the cause for improved confinement in this regime [3]. As most hybrid discharges have strong neutral beam heating, the central ion temperature is typically higher than the central electron temperature (T_{e0}). Plotted in Fig. 6

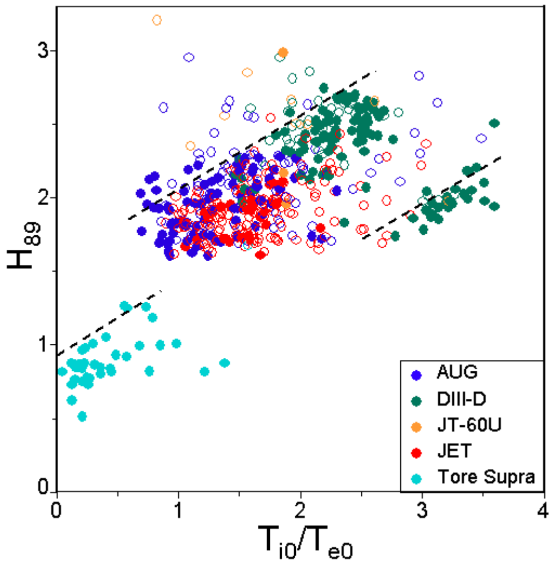

Figure 6: Confinement enhancement factor H_{89}, versus the ratio of the central ion (T_{i0}) and electron (T_{e0}) temperature. Transient (open symbols) and stationary results (closed symbols) are given.

is the confinement enhancement factor H_{89} versus the ratio T_{i0}/T_{e0}, for all experiments, without distinguishing between the different advanced scenarios. Stationary discharges show an improvement in confinement, with T_{i0}/T_{e0} for every experiment (plotting H_{89} versus central plasma rotation would show a similar trend). These results include QDB discharges on the right side of the plot (the green closed circles from DIII-D, using uncorrected values for H_{89}). The ratio T_{i0}/T_{e0} has been shown to be favourable to confinement for standard H-modes, as it is expected to stabilise drift wave turbulence. The net gain of the hybrid scenario when going to $T_{i0}/T_{e0} \rightarrow 1$, needs to be verified. In Fig. 6 the points at equal electron and ion temperature in the core are predominately obtained with neutral beam heating at high density. Recently, ASDEX Upgrade [7] has used ICRH in the core at low density, producing the highest confinement for conditions with $T_{i0} \approx T_{e0}$ in the database (blue closed circles at T_{i0}/T_{e0} ~1 and H_{89} >2). These results are corroborated by recent results from DIIII-D [8].

5. Performance limits

Advanced scenarios, in maximising the fraction of self-generated bootstrap current, are likely to operate near one or more stability limits. Discharges with reversed magnetic shear can gain in stability against ideal n = 1 modes by optimising the pressure profile and plasma shape [9]. The data in the database indicate that the achievable β_N is similar for the typical divertor plasmas used (average triangularity δ>0.2 and elongation κ>1.7), although a confirmation of operation at high β_N in a configuration matching the ITER shape would be desirable. The data support previous studies that the maximum β_N drops sharply for high pressure peaking (p_0/<p>, calculated using central density, central temperatures and stored energy, W), as shown in Fig. 7. This implies that reversed shear discharges with internal transport barriers that obtain higher pressure peaking compared to standard or hybrid scenarios have inherently a lower beta limit. In fact 80 % of the reversed shear discharges in the database achieve the high performance only transiently (duration <$10\tau_E$). Over the last ten years, more and more sophisticated control schemes have been devised to control reversed shear discharges with internal transport barriers, as to maximise the duration of the discharge at high beta.

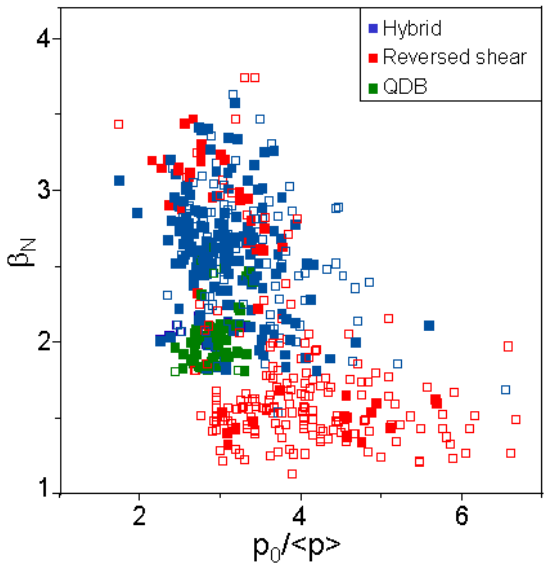

Figure 7: Normalised beta, β_N, as function of the pressure peaking, p_0/<p> for different advanced regimes. Transient (open symbols) and stationary results (closed symbols) are given.

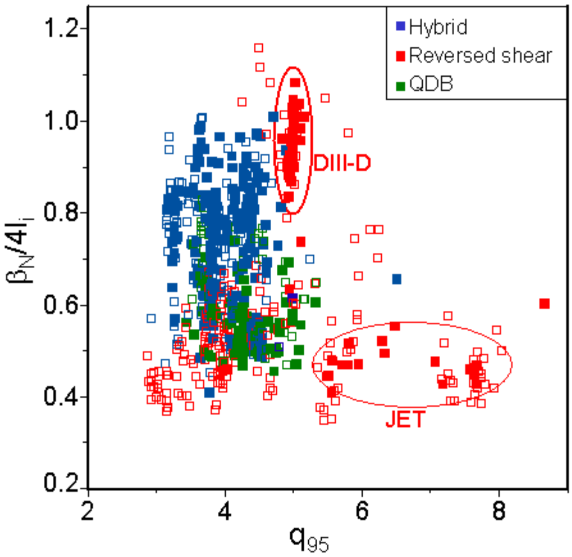

Figure 8: $\beta_N/4l_i$ versus q_{95}, the data are sorted for the different advanced regimes. Transient (open symbols) and stationary results (closed symbols) are given.

However, the operational diagram shown in Fig. 7 has not changed, demonstrating that broad pressure profiles are favourable for obtaining high beta. The data presented in this paper suggest that this implies operating without, or with weak internal transport barriers such that the central ion temperature is related to the edge ion temperature. The ratio of $\beta_N/4l_i$, indicative of the no-wall beta limit, is plotted versus q_{95} in Fig. 8. Hybrid scenarios operating with q_{95} in the range 3 to 4.5 obtain high beta values close to the no wall limit. Reversed shear discharges from DIII-D at q_{95}~5 even exceed this boundary by simultaneously stabilising resistive wall modes and avoiding neoclassical tearing modes (NTMs). At higher q_{95} values $\beta_N/4l_i$, drops substantially. Although, it is found that attainable no-wall β_N limit can fall with increasing q_{min}, typical for operation at high q_{95}, these discharges tend to operate at higher pressure peaking, hence their low beta limit is likely to be a culmination of both effects. The JET discharges shown in Fig. 8 operate with a low edge pedestal (type III ELMs) to maintain the internal transport barrier; experiments are planned at lower values for $q_{95,}$ using higher plasma shaping with broader pressure profiles.

6. Progress towards ITER

The discharges in the database show that the requirements for advanced operation in ITER can be met. For extrapolation towards ITER, dimensionless parameters such as the normalised collisionality ($\nu^* \sim a^7\langle n_e\rangle^3\kappa^2/\varepsilon^3W^2$, with $\langle n_e\rangle$ the average electron density) and normalised ion larmor radius ($\rho_i^* \equiv 0.00646\sqrt{\langle Ti\rangle}/(B_t a)$, with $\langle Ti\rangle$ the volume averaged ion temperature) are used. As most experiments are at low density, sustained by neutral beam fuelling alone, a lot of data points are close to the ν* values of the ITER reference scenario (using values given in [1]). In Fig. 9 the confinement improvement over ITER89P scaling is plotted versus ν^*/ν^*_{ITER}, together with the density peaking. Most discharges obtain peaked density profiles, predominantly near ITER ν* values. The confinement also reaches a maximum at low ν*. However, in the dataset the density peaking and H_{89} are not strongly correlated (cross correlation ~ 0.3 for all experiments). Clearly a comparison with standard H-modes would be desirable. This is the aim of future work in the ITPA groups.

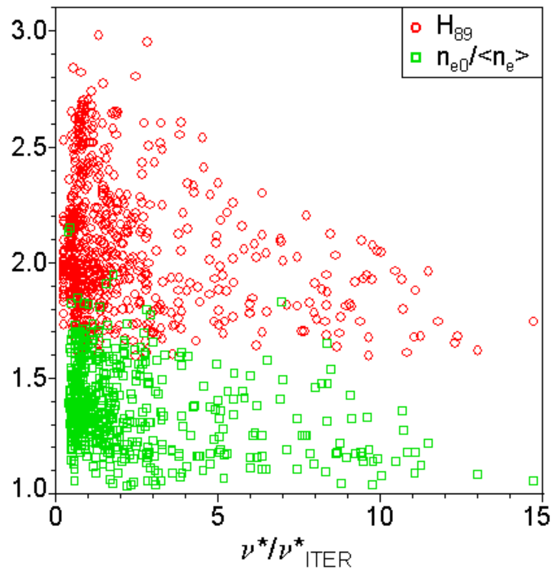

Figure 9: Confinement enhancement factor H_{89}, (red symbols) and the ratio of the central ion (T_{i0}) and electron (T_{e0}) temperature (green symbols), both are plotted versus the collisionality ν normalised to the ITER ν*.*

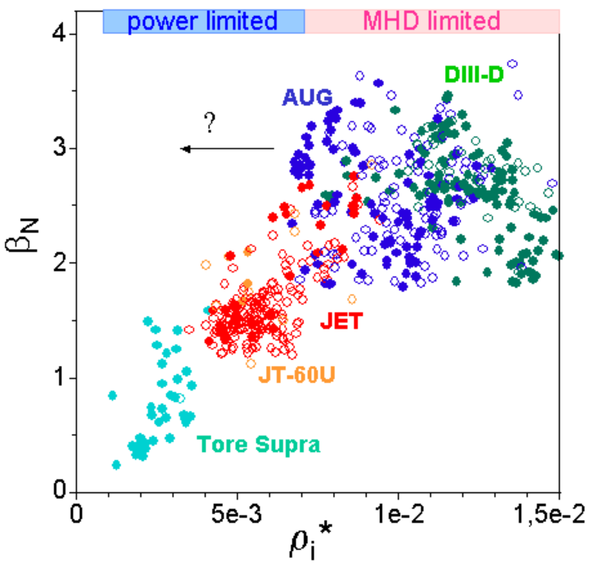

Figure 10: β_N plotted versus normalised ion larmor radius, ρ_i, for different experiments. Transient (open symbols) and stationary results (closed symbols) are given.*

Obtaining high beta at low normalised larmor radius is one of the main concerns for the ITER reference scenario since scaling of the occurrence of NTMs, triggered by seed islands provided by sawteeth, is unclear. Experiments documenting the scaling of the beta limit with ρ_i* for advanced regimes is desirable (ITER ρ_i* =1-2x10^{-3}). Recently, data has been plotted in a form shown in Fig. 10, were data from all experiments are included (here the data from Tore Supra are low ion temperature). While ASDEX Upgrade and DIII-D document the beta limit for this regime with β_N near 3, Fig. 10 gives the impression of a sharp drop in β_N going to low ρ_i*. In fact, the extrapolation to ITER remains unresolved since some experiments do not have sufficient input power to achieve β_N ~3 at their maximum toroidal field (Tore Supra, JT-60U and JET).

7. Conclusions

An international database is used to document the operation space and the performance of advanced scenarios. The hybrid scenario achieves stationary operation at high β_N ~3, operating at 50% non-inductive current fraction near the no wall beta limit (β_N ~ 4l_i). The confinement is improved over conventional H-modes, and increases with T_{i0}/T_{e0}. However, hybrid scenarios show a strong correlation between core and edge ion temperatures. For the reversed shear scenario, stationary operation has been obtained at $q_{95} \geq 5$, with the maximum in performance in line with ITER requirements for steady state operation at Q~5. A limitation to the achievable beta, set by the pressure peaking, only allows stationary operation for discharges with a similar strong correlation between core and edge ion temperature as observed for the hybrid regime. Both regimes predominantly operate close to ITER ν* values, achieving high confinement and peaked density profiles in this domain. The extrapolation of the results to lower ρ_i*, is hampered by a lack of input power in large experiments as they cannot achieve β_N ~3 at their maximum toroidal field (i.e. JET). From the analysis presented, collaboration experiments can be defined to better documentation the hybrid scenario operational space, to determine the beta limit in reversed shear discharges, to document core transport in relation to standard H-modes and to obtain discharges with equal ion and electron temperature. Furthermore, the compatibility of these regimes with divertor power handling and exhaust requirements in ITER should be assessed. Coordinated international experiments to investigate these issues can be expected to provide a more robust extrapolation to ITER.

References

[1] ITER Physics Basis *1999*, Nuclear Fusion **39** 2137.
[2] T. Fukuda et al *2001*, Proc. 28th EPS Conference (Funchal).
[3] J. Kinsey et al *2004*, this conference
[4] T. Fujita et al *2003*, 30th EPS Conference (St. Petersburg).
[5] X. Litaudon et al *2004*, Plasma Physics and Controlled Fusion 46 (2004).
[6] K.H. Burrell et al *2002* Plasma Physics and Controlled Fusion **44** A253.
[7] A. Stäbler et al *2004*, this conference.
[8] M. Wade et al *2004*, this conference.
[9] A. D. Turnbull et al *1998*, Nuclear Fusion **38** 1467.